

# Effect of imperfections and damping on the type of nonlinearity of circular plates and shallow spherical shells

Cyril Touzé, Cédric Camier, Gaël Favraud, Olivier Thomas

► **To cite this version:**

Cyril Touzé, Cédric Camier, Gaël Favraud, Olivier Thomas. Effect of imperfections and damping on the type of nonlinearity of circular plates and shallow spherical shells. *Mathematical Problems in Engineering*, Hindawi Publishing Corporation, 2008, 2008, pp.678307. <10.1155/2008/678307>. <hal-00838876>

**HAL Id: hal-00838876**

**<https://hal-ensta.archives-ouvertes.fr/hal-00838876>**

Submitted on 11 Mar 2016

**HAL** is a multi-disciplinary open access archive for the deposit and dissemination of scientific research documents, whether they are published or not. The documents may come from teaching and research institutions in France or abroad, or from public or private research centers.

L'archive ouverte pluridisciplinaire **HAL**, est destinée au dépôt et à la diffusion de documents scientifiques de niveau recherche, publiés ou non, émanant des établissements d'enseignement et de recherche français ou étrangers, des laboratoires publics ou privés.

# Effect of imperfections and damping on the type of non-linearity of circular plates and shallow spherical shells

Cyril Touzé<sup>(1)</sup>, Cédric Camier<sup>(1)</sup>, Gaël Favraud<sup>(1)</sup>, and Olivier Thomas<sup>(2)</sup>.

(1) ENSTA-UME, Unité de Mécanique, Chemin de la Hunière, 91761 Palaiseau Cedex, France, [cyril.touze@ensta.fr](mailto:cyril.touze@ensta.fr), [cedric.camier@ensta.fr](mailto:cedric.camier@ensta.fr), [gael.favraud@polytechnique.org](mailto:gael.favraud@polytechnique.org)

(2) CNAM, LMSSC, Laboratoire de Mécanique des structures et systèmes couplés, 2 rue Conté, 75003 Paris, France, [olivier.thomas@cnam.fr](mailto:olivier.thomas@cnam.fr)

---

**Abstract:** The effect of geometric imperfections and viscous damping on the type of non-linearity (*i.e.* the hardening or softening behaviour) of circular plates and shallow spherical shells with free edge, is here investigated. The Von Kármán large-deflection theory is used to derive the continuous models. Then, non-linear normal modes (NNMs), are used for predicting with accuracy the coefficient, the sign of which determines the hardening or softening behaviour of the structure. The effect of geometric imperfections, unavoidable in real systems, is studied by adding a static initial component in the deflection of a circular plate. Axisymmetric as well as asymmetric imperfections are investigated, and their effect on the type of non-linearity of the modes of an imperfect plate, is documented. Transitions from hardening to softening behaviour are predicted quantitatively for imperfections having the shapes of eigenmodes of a perfect plate. The role of 2:1 internal resonance in this process is underlined. When damping is included in the calculation, it is found that the softening behaviour is generally favoured, but its effect remains limited.

*Keywords:* hardening/softening behaviour, spherical shells, circular plates, geometric imperfections, damping.

---

## 1 Introduction

When continuous structures such as plates and shells undergo large amplitude motions, the geometrical non-linearity leads to a dependence of free oscillation frequencies on vibration amplitude. The type of non-linearity describes this dependency, which can be of the hardening type (the frequency increases with amplitude), or of the softening type (the frequency decreases). A large amount of literature is devoted to predicting this type of non-linearity for continuous structures, and especially for structures with an initial curvature such as arches or shells, because the presence of the

quadratic non-linearity makes the problem more difficult to solve. On the other hand, the hardening behaviour of flat structures such as beams and plates is a clearly established fact, on the theoretical as well as the experimental viewpoint, see *e.g.* [1, 2, 3, 4, 5, 6]. The presence of the quadratic non-linearity may change the behaviour from hardening to softening type, depending on the relative magnitude of quadratic and cubic non-linear terms.

Among the available studies concerned with this subject, quite all of them that were published before 1992 could not be considered as definitive since they generally restrict to the case of a single-mode vibration through Galerkin method, see for example [7, 8, 9] for shallow spherical shells, or [10] for imperfect circular plates. Unfortunately, it has been shown by a number of more recent investigations that too severe truncations lead to erroneous results in the prediction of the type of non-linearity, see for example [11, 12], or the abundant literature on circular cylindrical shells, where the investigators faced this problem for a long time [13, 14, 15, 16, 17, 18]. As a consequence, a large number of modes must mandatory be kept in the truncation of the Partial Differential Equations (PDEs) of motion, in order to accurately predict the type of non-linearity. Recent papers are now available where a reliable prediction is realized, for the case of buckled beams [19], circular cylindrical shells [20], suspended cables [21] and shallow spherical shells [22].

However, these last studies are restricted to the case of perfect structures, and the damping is neglected in the computations; and both of them have an influence on the type of non-linearity, so that a complete and thorough theoretical study that could be applied to real structures need to address the effect of imperfections and damping. The geometric imperfections have a first-order effect on the linear as well as the non-linear characteristics of structures. A large amount of studies are available, where the effect of imperfections on the eigenfrequencies and on the buckling loads, are generally addressed, see for example [23, 24, 25, 26, 27, 28] for the case of circular cylindrical shells, [29] for shallow cylindrical panels, [30] for the case of rectangular plates. Non-linear frequency-responses curves are shown in [31, 32] for clamped circular plates, [33, 34, 35] for rectangular plates, [36] for circular cylindrical shells, and [37] for circular cylindrical panels. Even though the presence of geometric imperfection has been recognized as a major factor that could make the hardening behaviour of the flat plate turn to softening behaviour for an imperfection amplitude of a fraction of the plate thickness [10, 38], a quantitative study, which is not restricted to axisymmetric modes and that does not perform too crude truncations in the Galerkin expansion, is still missing.

To the authors' knowledge, the role of the damping in the prediction of the type of non-linearity has been only recently detected as an important factor that could change the behaviour from hardening to softening type [39]. In particular, it is shown in [39] on a simple two degrees-of-freedom (dofs) system, that the damping generally favours the softening behaviour. The aim of the present study is thus to apply this theoretical result to the practical case of a damped shallow spherical shell, so as to quantitatively assess the effect of structural damping of the viscous type on the type of non-linearity of a two-dimensional vibrating structure.

The article is organized as follows. In section 2, local equations and boundary conditions for an imperfect circular plate with free edge, are given. Then the method used for computing the type of non-linearity is explained. Section 3 investigates how typical imperfections may turn the hardening behaviour of flat plates to softening behaviour. Quantitative results are given for selected imperfections having the shape of eigenmodes of the perfect structure. Section 4 is devoted to the effect of viscous damping. The particular case of a spherical imperfection is selected, and the results are shown for three different damping dependances on frequency.

## 2 Theoretical formulation

### 2.1 Local equations and boundary conditions

A thin plate of diameter  $2a$  and uniform thickness  $h$  is considered, with  $h \ll a$ , and free-edge boundary condition. The local equations governing the large-amplitude displacement of a perfect plate, assuming the non-linear Von Kármán strain-displacement relationship and neglecting in-plane inertia, are given for example in [40, 5]. An initial imperfection, denoted by  $w_0(r, \theta)$  and associated with zero initial stresses is also considered, see Fig. 1. The shape of this imperfection is arbitrary, and its amplitude is small compared to the diameter (shallow assumption):  $w_0(r, \theta) \ll a$ . The local equations for an imperfect plate deduce from the perfect case [41, 18, 42]. With  $w(r, \theta, t)$  being the transverse displacement from the imperfect position at rest, the equations of motion write:

$$D\Delta\Delta w + \rho h \ddot{w} = L(w, F) + L(w_0, F) - c\dot{w}, \quad (1a)$$

$$\Delta\Delta F = -\frac{Eh}{2} [L(w, w) + 2L(w, w_0)], \quad (1b)$$

where  $D = \frac{Eh^3}{12(1-\nu^2)}$  is the flexural rigidity,  $\Delta$  stands for the laplacian operator,  $c$  accounts for structural damping of the viscous type,  $F$  is the Airy stress function, and  $L$  is a bilinear operator, whose expression in polar co-ordinates reads:

$$L(w, F) = w_{,rr} \left( \frac{F_{,r}}{r} + \frac{F_{,\theta\theta}}{r^2} \right) + F_{,rr} \left( \frac{w_{,r}}{r} + \frac{w_{,\theta\theta}}{r^2} \right) - 2 \left( \frac{w_{,r\theta}}{r} - \frac{w_{,\theta}}{r^2} \right) \left( \frac{F_{,r\theta}}{r} - \frac{F_{,\theta}}{r^2} \right). \quad (2)$$

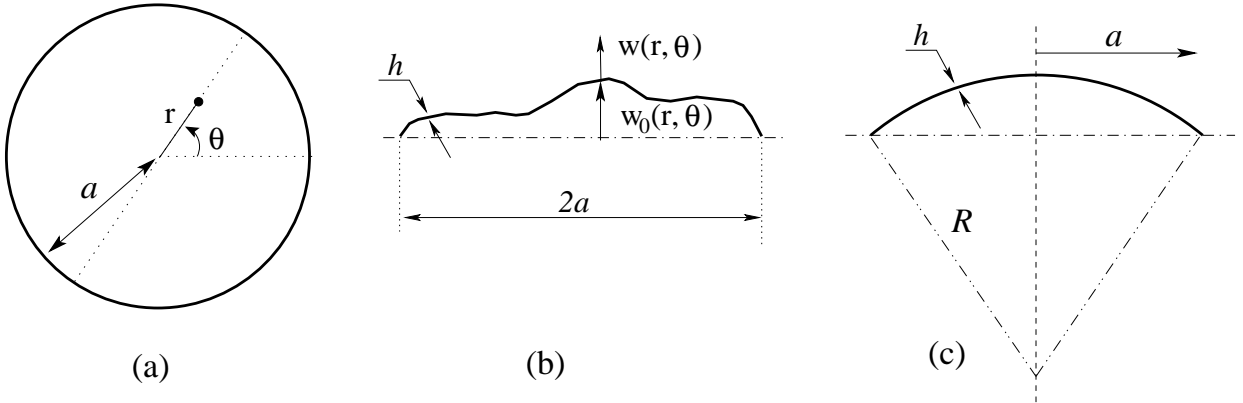


Figure 1: (a) Top view and (b) cross-section of an imperfect circular plate of radius  $a$  and thickness  $h$ . (c) The particular case of a spherical imperfection, with radius of curvature  $R$ .

The equations are then written with non-dimensional variables, by introducing:

$$r = a\bar{r}, \quad t = a^2\sqrt{\rho h/D}\bar{t}, \quad w = h\bar{w}, \quad w_0 = h\bar{w}_0 \quad (3)$$

$$F = Eh^3\bar{F}, \quad c = [Eh^3/a^2]\sqrt{\rho h/D}\bar{c}. \quad (4)$$

As non-dimensional equations will be used in the remainder of the study, overbars are now omitted

in order to write the dimensionless form of the equations of motion:

$$\Delta\Delta w + \ddot{w} = \varepsilon [L(w, F) + L(w_0, F) - c\dot{w}], \quad (5a)$$

$$\Delta\Delta F = -\frac{1}{2} [L(w, w) + 2L(w, w_0)], \quad (5b)$$

where  $\varepsilon = 12(1 - \nu^2)$ .

The boundary conditions for the case of a free edge write, in non-dimensional form [5]:

$$F_{,r} + F_{,\theta\theta} = 0, \quad F_{,r\theta} + F_{,\theta} = 0, \quad \text{at } r = 1 \quad (6a)$$

$$w_{,rr} + \nu w_{,r} + \nu w_{,\theta\theta} = 0, \quad \text{at } r = 1 \quad (6b)$$

$$w_{,rrr} + w_{,rr} - w_{,r} + (2 - \nu)w_{,r\theta\theta} - (3 - \nu)w_{,\theta\theta} = 0, \quad \text{at } r = 1. \quad (6c)$$

In order to discretize the PDEs, a Galerkin procedure is used. As the eigenmodes can not be computed analytically because the shape of the imperfection is arbitrary, the eigenmodes of the perfect plate  $\Psi_p(r, \theta)$  are selected as basis functions. Analytical expressions of  $\Psi_p(r, \theta)$  involve Bessel functions and can be found in [5]. The unknown displacement is expanded with:

$$w(r, \theta, t) = \sum_{p=1}^{+\infty} q_p(t) \Psi_p(r, \theta), \quad (7)$$

where the time functions  $q_p$  are now the unknowns. In this expression, the subscript  $p$  refers to a specific mode of the perfect plate, defined by a couple  $(k, n)$ , where  $k$  is the number of nodal diameters and  $n$  the number of nodal circles. If  $k \neq 0$ , a binary variable is added, indicating the preferential configuration considered (*sine* or *cosine* companion mode). Inserting the expansion (7) into Eqs. (5), and using the orthogonality properties of the expansion functions, the dynamical equations are found to be, for all  $p = 1 \dots N$ :

$$\ddot{q}_p + 2\xi_p\omega_p\dot{q}_p + \varepsilon \left[ \sum_{i=1}^{+\infty} \alpha_i^p q_i + \sum_{i,j=1}^{+\infty} \beta_{ij}^p q_i q_j + \sum_{i,j,k=1}^{+\infty} \Gamma_{ijk}^p q_i q_j q_k \right] = 0. \quad (8)$$

Linear coupling terms between the oscillator equations are present, as the natural modes have not been used for discretizing the PDEs. Analytical expressions of the coupling coefficients  $(\alpha_i^p, \beta_{ij}^p, \Gamma_{ijk}^p)$  are given in [42]. The generic viscous damping term  $c$  of Eq. (5a) has been specialized in the discretized equations so as to handle the more general case of a modal viscous damping term of the form  $2\xi_p\omega_p\dot{q}_p$ , where  $\xi_p$  is the damping factor and  $\omega_p$  the eigenfrequency of mode  $p$ . On the other hand, external forces have been cancelled, as the remainder of the study will consider free vibrations only.

In order to work with diagonalized linear parts, the matrix of eigenvectors  $\mathbf{P}$  of the linear part  $\mathbf{L} = [\alpha_i^p]_{p,i}$ , is numerically computed. A linear change of co-ordinates is processed,  $\mathbf{q} = \mathbf{P}\mathbf{X}$ , where  $\mathbf{X} = [X_1 \dots X_N]^T$  is, by definition, the vector of modal co-ordinates, and  $N$  is the number of expansion function kept in practical application of the Galerkin's method. Application of  $\mathbf{P}$  makes the linear part diagonal, so that the discretized equations of motion finally writes,  $\forall p = 1 \dots N$ :

$$\ddot{X}_p + 2\xi_p\omega_p\dot{X}_p + \omega_p^2 X_p + \varepsilon \left[ \sum_{i,j=1}^N g_{ij}^p X_i X_j + \sum_{i,j,k=1}^N h_{ijk}^p X_i X_j X_k \right] = 0. \quad (9)$$

The temporal equations (9) describe the dynamics of an imperfect circular plate. The type of non-linearity can be inferred from these equations. Unfortunately, too severe truncations in (9), *e.g.* by keeping only one dof ( $N = 1$ ) when studying the non-linear behaviour of the  $p^{th}$  mode, lead to incorrect predictions. Non-linear normal modes (NNMs) offer a clean framework for deriving a single oscillator equation capturing the correct type of non-linearity [12]. This is recalled in the next section, where the analytical expression of the coefficient dictating the type of non-linearity is given.

## 2.2 Type of non-linearity

Non-linear oscillators differ from linear ones by the frequency dependence on vibration amplitude. The type of non-linearity defines the behaviour, which can be of the hardening or the softening type.

As shown in [12], NNMs provides an efficient framework for properly truncating non-linear oscillator equations like (9) and predict the type of non-linearity (hardening or softening behaviour). The method has already been successfully applied to the case of undamped shallow spherical shells in [22]. The main idea is to derive a non-linear change of co-ordinates, allowing one to pass from the *modal*  $X_p$  co-ordinates to new-defined *normal* co-ordinates  $R_p$ , describing the motions in an invariant-based span of the phase space. The non-linear change of co-ordinates is computed from Poincaré and Poincaré-Dulac's theorems, by successive elimination of non-essential coupling terms in the non-linear oscillator equations. Formally, it reads:

$$\begin{aligned} X_p = R_p &+ \sum_{i=1}^N \sum_{j \geq i}^N (a_{ij}^p R_i R_j + b_{ij}^p S_i S_j) + \sum_{i=1}^N \sum_{j=1}^N c_{ij}^p R_i S_j \\ &+ \sum_{i=1}^N \sum_{j \geq i}^N \sum_{k \geq j}^N (r_{ijk}^p R_i R_j R_k + s_{ijk}^p S_i S_j S_k) \\ &+ \sum_{i=1}^N \sum_{j=1}^N \sum_{k \geq j}^N (t_{ijk}^p S_i R_j R_k + u_{ijk}^p R_i S_j S_k), \end{aligned} \quad (10a)$$

$$\begin{aligned} Y_p = S_p &+ \sum_{i=1}^N \sum_{j \geq i}^N (\alpha_{ij}^p R_i R_j + \beta_{ij}^p S_i S_j) + \sum_{i=1}^N \sum_{j=1}^N \gamma_{ij}^p R_i S_j \\ &+ \sum_{i=1}^N \sum_{j \geq i}^N \sum_{k \geq j}^N (\lambda_{ijk}^p R_i R_j R_k + \mu_{ijk}^p S_i S_j S_k) \\ &+ \sum_{i=1}^N \sum_{j=1}^N \sum_{k \geq j}^N (\nu_{ijk}^p S_i R_j R_k + \zeta_{ijk}^p R_i S_j S_k) \end{aligned} \quad (10b)$$

A third-order approximation of the complete change of co-ordinates is thus computed. The analytical expressions of the introduced coefficients  $\{a_{ij}^p, b_{ij}^p, c_{ij}^p, r_{ijk}^p, s_{ijk}^p, t_{ijk}^p, u_{ijk}^p, \}$ , and  $\{\alpha_{ij}^p, \beta_{ij}^p, \gamma_{ij}^p, \lambda_{ijk}^p, \mu_{ijk}^p, \nu_{ijk}^p, \zeta_{ijk}^p, \}$  are not given here for the sake of brevity. The interested reader may find them in [12] for the undamped case, and in [39] for the damped case.

Once the non-linear change of co-ordinates operated, proper truncations can be realized. In particular, keeping only the normal co-ordinates  $R_p$  allows prediction of the correct type of non-linearity for the  $p^{th}$  mode. The dynamics onto the  $p^{th}$  NNM reads:

$$\ddot{R}_p + \omega_p^2 R_p + 2\xi_p \omega_p \dot{R}_p + (\varepsilon h_{ppp}^p + A_{ppp}^p) R_p^3 + B_{ppp}^p R_p \dot{R}_p^2 + C_{ppp}^p R_p^2 \dot{R}_p = 0, \quad (11)$$

where  $A_{ppp}^p$ ,  $B_{ppp}^p$ , and  $C_{ppp}^p$  are new coefficients coming from the change of co-ordinates. Their expressions involve the quadratic coefficients  $\{g_{ij}^p\}$  only, together with some of the transformation coefficients,  $\{a_{ij}^p, b_{ij}^p, c_{ij}^p\}$  from Eqs (10) [39]:

$$A_{ppp}^p = \varepsilon \left[ \sum_{l \geq i}^N g_{pl}^p a_{pp}^l + \sum_{l \leq i} g_{lp}^p a_{pp}^l \right], \quad (12a)$$

$$B_{ppp}^p = \varepsilon \left[ \sum_{l \geq i}^N g_{pl}^p b_{pp}^l + \sum_{l \leq i} g_{lp}^p b_{pp}^l \right], \quad (12b)$$

$$C_{ppp}^p = \varepsilon \left[ \sum_{l \geq i}^N g_{pl}^p c_{pp}^l + \sum_{l \leq i} g_{lp}^p c_{pp}^l \right]. \quad (12c)$$

The asymptotic third-order approximation of the dynamics onto the  $p^{\text{th}}$  NNM given by Eq. (11) allows one to accurately predict the type of non-linearity of mode  $p$ . A first-order perturbative development from Eq. (11) gives the dependence of the non-linear oscillation frequency  $\omega_{NL}$  on the amplitude of vibration  $a$  by the relationship:

$$\omega_{NL} = \omega_p(1 + T_p a^2), \quad (13)$$

where  $\omega_p$  is the natural angular frequency. In this expression,  $T_p$  is the coefficient governing the type of non-linearity. If  $T_p > 0$ , then hardening behaviour occurs, whereas  $T_p < 0$  implies softening behaviour. The analytical expression for  $T_p$  writes [12, 22]:

$$T_p = \frac{1}{8\omega_p^2} \left[ 3(A_{ppp}^p + \varepsilon h_{ppp}^p) + \omega_p^2 B_{ppp}^p \right], \quad (14)$$

Finally, the method used for deriving the type of non-linearity can be summarized as follows. For a geometric imperfection of a given amplitude, the discretization leading to the non-linear oscillator equations (9) is first computed. The numerical effort associated to this operation is the most important but remains acceptable on a standard computer. Then the non-linear change of co-ordinates is computed, which allows derivation of the  $A_{ppp}^p$  and  $B_{ppp}^p$  terms occurring in Eq. (14), the sign of which determines the type of non-linearity. Numerical results are given in the next section for specific imperfections.

### 3 Effect of imperfections

This section is devoted to numerical results about the effect of typical imperfections on the type of non-linearity of imperfect plates. Two typical imperfections are selected. The first one is axisymmetric and has the shape of mode (0,1), the second one has the shape of the first asymmetric mode (2,0). Consequently, damping is not considered, so that in each equation we have:  $\forall p = 1 \dots N, \xi_p = 0$ . The study of the effect of damping will be done separately and is postponed to section 4.

#### 3.1 Axisymmetric imperfection

In this section, the particular case of an axisymmetric imperfection having the shape of mode (0,1) (*i.e.* with one nodal circle and no nodal diameter), is considered. The expression of the static



deflection writes:

$$w_0(r) = a_{(0,1)}\Psi_{(0,1)}(r), \quad (15)$$

where  $\Psi_{(0,1)}(r)$  is the mode shape, depending only on the radial co-ordinate  $r$  as a consequence of axisymmetry, and  $a_{(0,1)}$  the considered amplitude. The mode shape  $\Psi_{(0,1)}(r)$  depends on Bessel function [5], and is shown in Fig. 2. The eigenmode is normalized so that  $\int_0^1 \Psi_{(0,1)}^2(r)dr = 1$ .

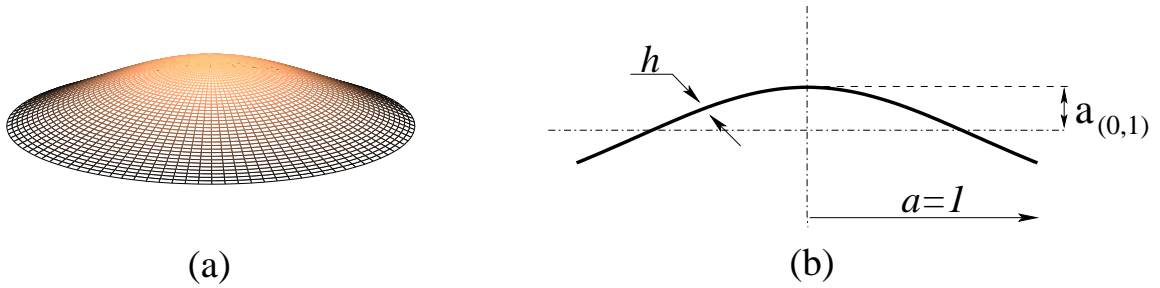


Figure 2: (a) Three-dimensional view and (b) cross-section of the circular plate with geometric imperfection having the shape of the first axisymmetric mode. As non-dimensional quantities are used,  $a = 1$  and the amplitude  $a_{(0,1)}$  of the imperfection is made non-dimensional with respect to the thickness  $h$ .

Fig. 3 shows the effect of the imperfection on the eigenfrequencies, for an imperfection amplitude from 0 (perfect plate) to  $10h$ . It is observed that the purely asymmetric modes  $(k, 0)$ , having no nodal circle and  $k$  nodal diameters, are marginally affected by the axisymmetric imperfection. The computation has been done by keeping 51 basis functions: purely asymmetric modes from  $(2,0)$  to  $(10,0)$ , purely axisymmetric modes from  $(0,1)$  to  $(0,13)$  and mixed modes from  $(1,1)$  to  $(6,1)$ ,  $(1,2)$ ,  $(2,2)$ ,  $(3,2)$  and  $(1,3)$ . More details and comparisons with a numerical solution based on finite elements are provided in [42, 43]. The slight dependence of purely asymmetric eigenfrequencies on an axisymmetric imperfection has already been observed in [44] with the case of the shallow spherical shell.

First, the effect of the imperfection on the axisymmetric modes  $(0,1)$  and  $(0,2)$  is studied. In this case the problem is fully axisymmetric so that all the truncations can be limited to axisymmetric modes only, which drastically reduces the numerical burden. The result for mode  $(0,1)$  is shown in Fig. 4. It is observed that the huge variation of the eigenfrequency with respect to the amplitude of the imperfection results in a quick turn of the behaviour from the hardening to the softening type, occurring for an imperfection amplitude of  $a_{(0,1)} = 0.38h$ . This small value has direct implication for the case of real plates. As the behaviour changes for a fraction of the plate thickness, it should not be intriguing to measure a softening behaviour with real plates having small imperfections. This result can also be compared to an earlier result obtained by Hui [10]. Although Hui did not study free edge boundary condition, he reported a numerical result for the case of simply supported boundary conditions, where the behaviour changes for an imperfection amplitude of  $0.28h$ . The second main observation inferred from Fig. 4 is the occurrence of 2:1 internal resonance between eigenfrequencies, leading to discontinuities in the coefficient  $T_{(0,1)}$  dictating the type of non-linearity. This fact



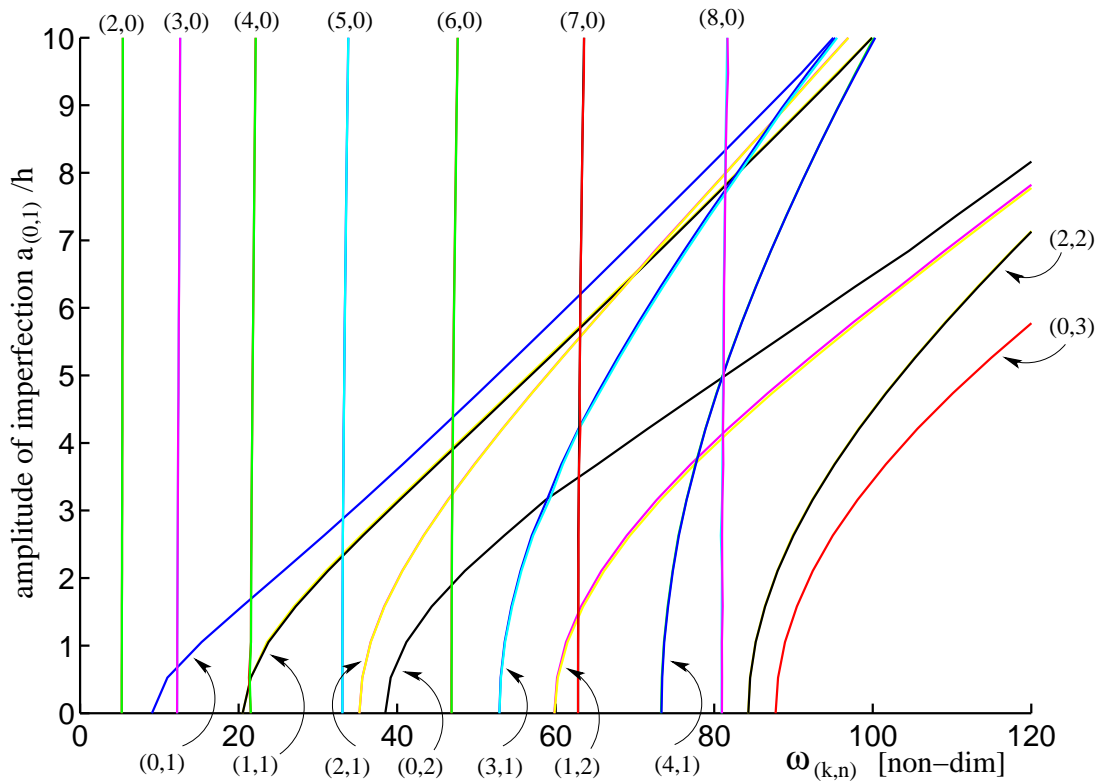


Figure 3: Non-dimensional natural frequencies  $\omega_{(k,n)}$  of the imperfect plate versus the amplitude of the imperfection having the shape of mode (0,1).

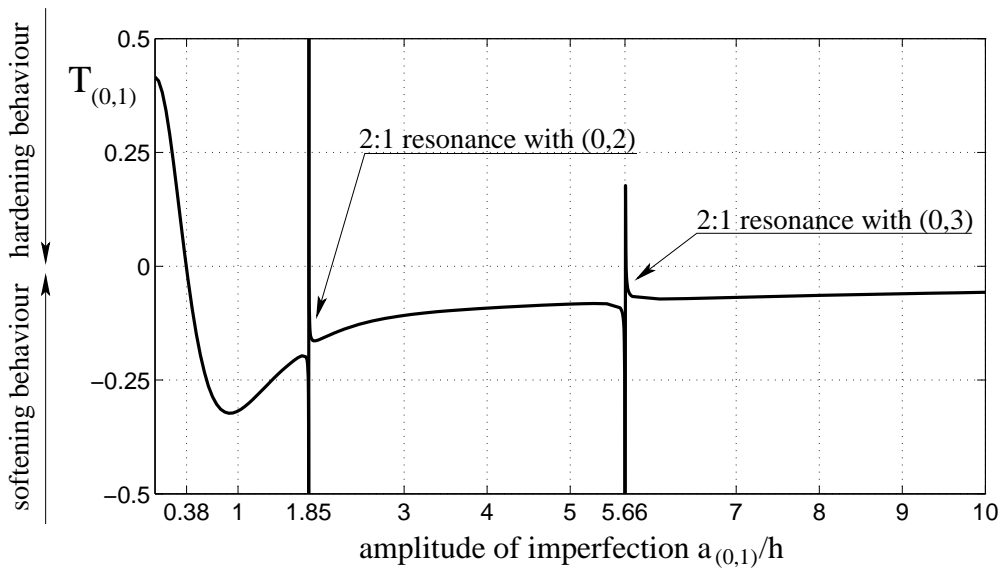


Figure 4: Type of non-linearity for mode (0,1) with an axisymmetric imperfection having the shape of mode (0,1).

has already been observed and commented for the case of shallow spherical shells in [22]. It has also been observed for buckled beams and suspended cables [19, 21]. This is a small denominator effect typical of internal resonance, *i.e.* when the frequency of the studied mode (0,1) exactly fulfills the relationship  $2\omega_{(0,1)} = \omega_{(0,n)}$  with another axisymmetric mode. 2:1 resonance arises here with mode (0,2) at  $1.85h$  and with mode (0,3) at  $5.66h$ . On a practical point of view, one must bear in mind that when 2:1 internal resonance occurs, single-mode solution does not exist anymore, only coupled solutions are possible. Hence the concept of the type of non-linearity, intimately associated with a single dof behaviour, loses its meaning in a narrow interval around the resonance.

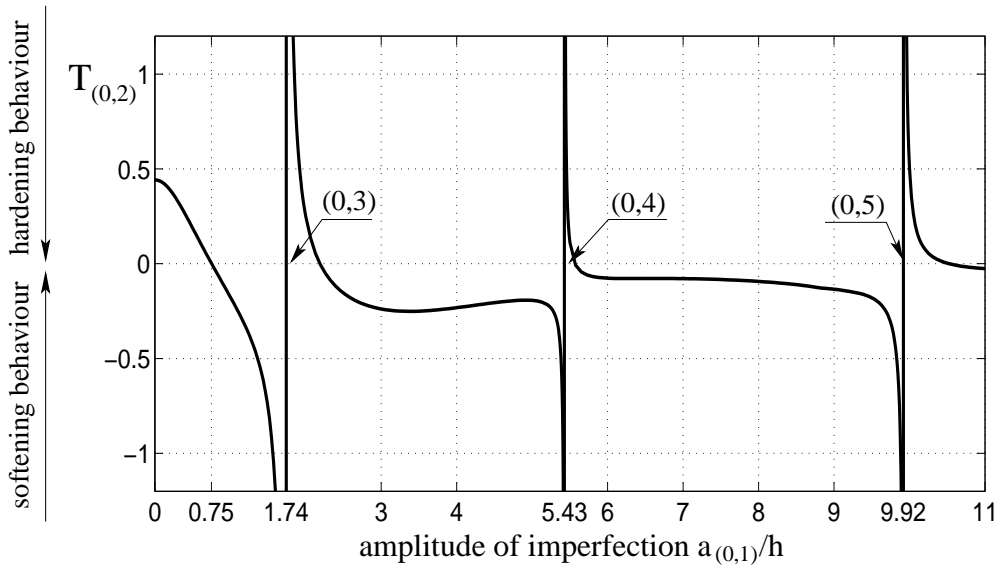


Figure 5: Type of non-linearity for mode (0,2) with an axisymmetric imperfection having the shape of mode (0,1). 2:1 internal resonances with modes (0,3), (0,4) and (0,5) occurs respectively for  $a_{(0,1)}/h = 1.74, 5.43$  and  $9.92$ .

The numerical result for mode (0,2) is shown in Fig. 5. Once again, the geometric effect is important and leads to a change of behaviour occurring at  $a_{(0,1)} = 0.75h$ , *i.e.* for a small level of imperfection. 2:1 internal resonance also occurs, thus creating narrow region where hardening behaviour could be observed. This result extends Hui's analysis since only mode (0,1) was studied. Moreover, as a single-mode truncation were used in [10], 2:1 resonances were missed.

Finally, the effect of the imperfection on asymmetric modes is shown in Fig. 6 for modes (2,0) and (4,0). The very slight variation of the eigenfrequencies of these modes versus the axisymmetric imperfection results in a very slight effect of the geometry. It is observed that before the first 2:1 internal resonance, the type of non-linearity shows small variations. Hence, it is the behaviour of the other eigenfrequencies and the occurrence of 2:1 internal resonance that makes, in these cases, the behaviour turn from hardening to softening behaviour. For mode (2,0) this occurs for an imperfection amplitude of  $a_{(0,1)} = 0.44h$ , where 2:1 resonance with mode (0,1) is observed. For mode (4,0), the first 2:1 resonance occurs with mode (0,2) at  $a_{(0,1)} = 1.39h$ , but do not change the behaviour. It is the resonance with mode (0,1) at  $a_{(0,1)} = 4h$  which makes the behaviour turn from hardening to softening.

These results corroborate those obtained on shallow spherical shells [22]. The fundamental importance of axisymmetric modes in the study of asymmetric ones is confirmed, showing once

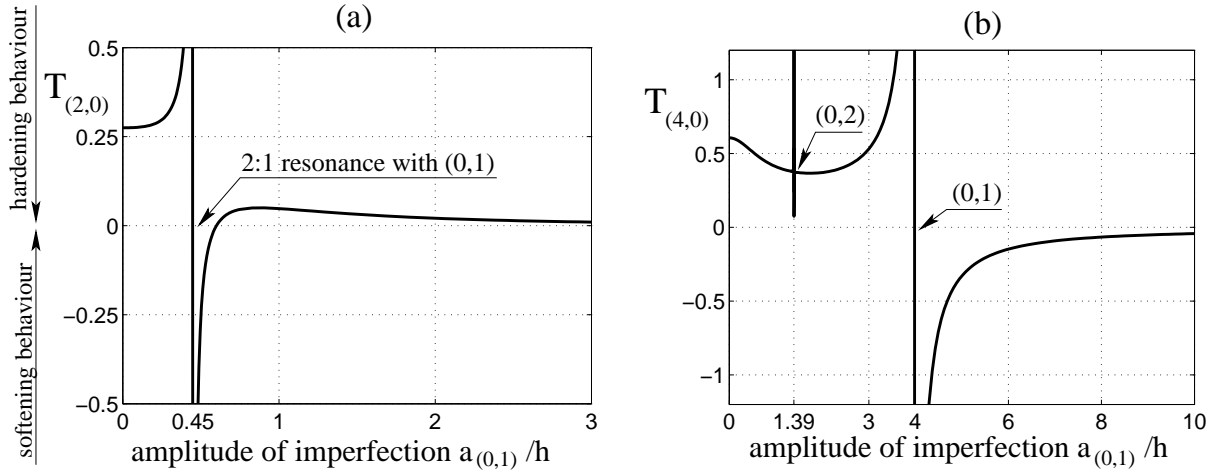


Figure 6: Type of non-linearity for (a): mode (2,0), and (b): mode (4,0), with an axisymmetric imperfection having the shape of mode (0,1).

again that reduction to single mode has no chance to deliver correct results. The behaviour of purely asymmetric modes is found to be of the hardening type until the 2:1 internal resonance with mode (0,1) occurs. However, a specificity of mode (2,0) with regard to all the other purely asymmetric modes is that after this resonance, hardening behaviour (though with a very small value of  $T_{(2,0)}$ ), is observed. This was also the case for shallow spherical shells [22]. Finally, for very large values of the imperfection, the behaviour tends to be neutral.

### 3.2 Asymmetric imperfection

In this section, the effect of an imperfection having the shape of mode (2,0), is studied. Due to the loss of symmetry, degenerated modes are awaited to cease to exist : the equal eigenfrequencies of the *sine* and *cosine* configuration of degenerated modes split. In the following, distinction is made systematically between the sine or cosine configuration of companion modes, *e.g.* mode (2,0,C) (resp (2,0,S)) refers to the cosine (resp. sine) configuration. More precisely, the imperfection has the shape of (2,0,C), and is shown in Fig. 7.

The behaviour of the eigenfrequencies with the imperfection is shown in Fig. 8. As expected, the variation of the eigenfrequency corresponding to (2,0,C) is huge whereas (2,0,S) keep quite a constant value. The symmetry is not completely broken. One can show that only eigenmodes of the type  $(2k, n)$  split. On the other hand, as shown in Fig. 8, modes (3,0), (5,0), (1,1) are still degenerated.

The numerical results for type of non-linearity relative to the two configurations (2,0,C) and (2,0,S), are shown in Fig. 9. The natural frequency of mode (2,0,C) undergoes a huge variation, which result in a quick change of behaviour, occurring at  $0.54h$ . Then, a 2:1 internal resonance with (0,2) is noted, but without a noticeable change in the type of non-linearity, as the interval where the discontinuity is present is very narrow. In this case, the behaviour of  $T_{(2,0,C)}$  looks like the one observed in the precedent case, *i.e.* the variation of  $T_{(0,1)}$  versus an imperfection having the same shape. On the other hand, the eigenfrequency of mode (2,0,S) remains quite unchanged, so that the behaviour of  $T_{(2,0,S)}$  is not much affected by the imperfection, until the 2:1 internal resonance is

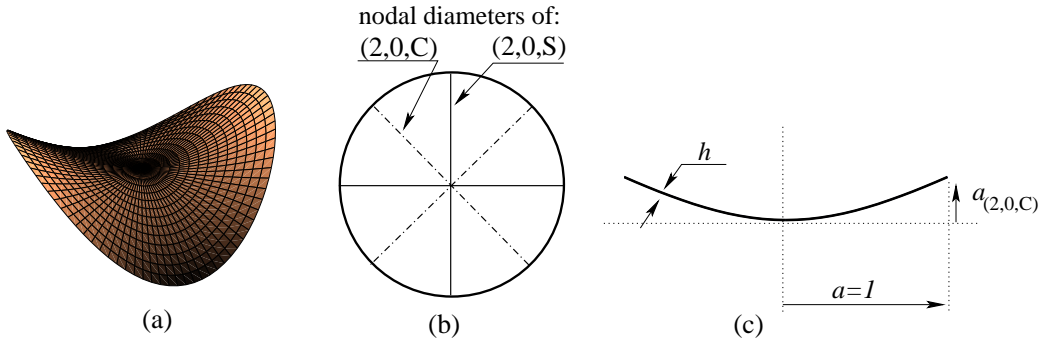


Figure 7: (a) 3-d view, (b) top view and (c) cross-section along  $\theta = 0$  for the plate with imperfection having the shape of mode (2,0,C).

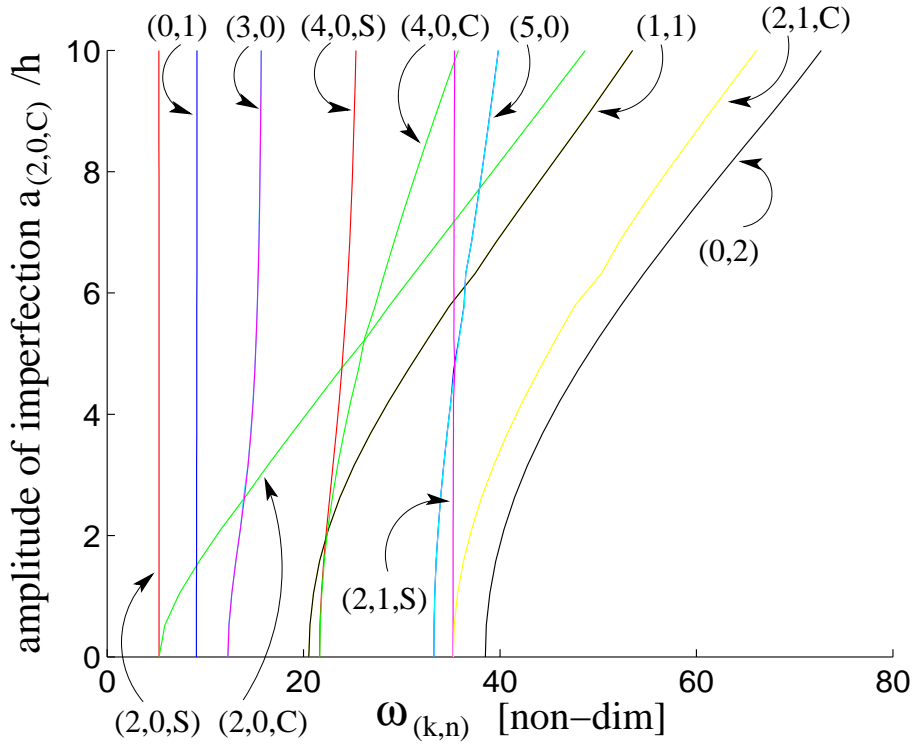


Figure 8: Non-dimensional natural frequencies  $\omega_{(k,n)}$  of the imperfect plate versus the amplitude of the imperfection having the shape of mode (2,0,C).

encountered. In that case, the resonance occurs with the other configuration, *i.e.* mode (2,0,C).

Finally, the results for the first two axisymmetric modes (0,1) and (0,2) are shown in Fig. 10. Mode (0,1) shows a very slight variation of its eigenfrequency with respect to the asymmetric imperfection (2,0,C). Consequently, the type of non-linearity is not much affected, until the eigenfrequency of (2,0,C) comes to two times  $\omega_{(0,1)}$ : 2:1 internal resonance occurs, and the behaviour becomes softening. On the other hand, the eigenfrequency of (0,2) is more affected by the imperfection. This result in an important decrease of  $T_{(0,2)}$  while still remaining positive. A 2:1 internal resonance with (0,3) is encountered for  $3.51h$ , and two others 2:1 resonance, with (0,4) and (0,5), occurs around  $8h$ .

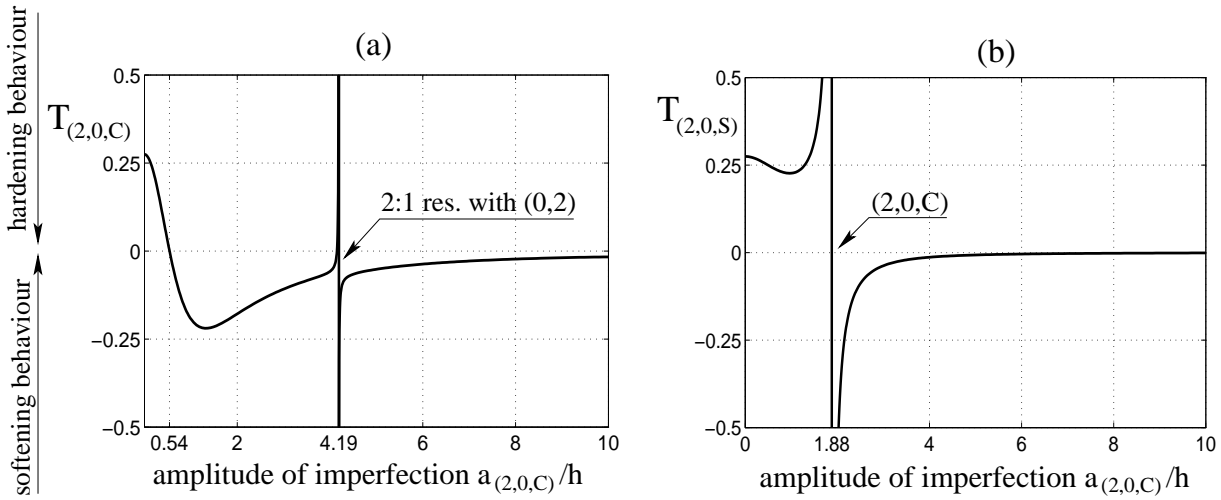


Figure 9: Type of non-linearity for (a): mode (2,0,C) and (b): (2,0,S); for an imperfection having the shape of mode (2,0,C).

However the interval on which the type of non-linearity changes its sign is so narrow that it can be neglected. The behaviour is thus mainly of the hardening type for (0,2).

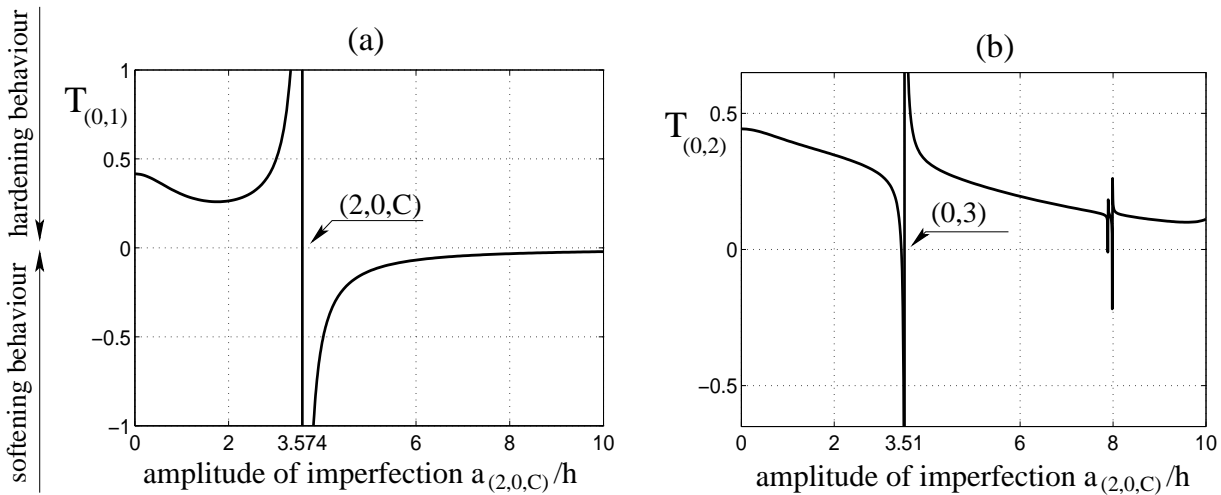


Figure 10: Type of non-linearity for (a): mode (0,1) and (b): (0,2); for an imperfection having the shape of mode (2,0,C).

## 4 Effect of damping

In this section, the effect of viscous damping on the type of non-linearity, is addressed. The particular case of the shallow spherical shell is selected to establish the results. The equations of motion are first briefly recalled. Then specific cases of damping are considered, hence complementing the results of [22], that were limited to the undamped shell.

## 4.1 The shallow spherical shell equations

The local equations of motions for the shallow spherical shell can be obtained directly, see [44] for a thorough presentation. They can also be obtained from Eqs (5), by selecting an imperfection having a spherical shape, as shown in Fig. 1(c), see [42]. With  $R$  the radius of curvature of the spherical shell ( $R \gg a$  to fulfill the shallow assumption), the local equations write [44]:

$$\Delta\Delta w + \varepsilon_q \Delta F + \ddot{w} = \varepsilon [L(w, F) - c\dot{w} + p(r, \theta, t)], \quad (16a)$$

$$\Delta\Delta F - \sqrt{\kappa}\Delta w = -\frac{1}{2}L(w, w), \quad (16b)$$

where the aspect ratio  $\kappa$  of the shell has been introduced:

$$\kappa = \frac{a^4}{R^2 h^2}, \quad (17)$$

and  $\varepsilon_q = 12(1 - \nu^2)\sqrt{\kappa}$ . The boundary conditions for the case of the spherical shell with free edge write exactly as in the case of the imperfect circular plates so that Eqs (6) are still fulfilled [44, 42]. A peculiarity of the spherical shell is that all the involved quantities, linear (eigenfrequencies and mode shapes) and non-linear (coupling coefficients and type of non-linearity) only depends on  $\kappa$ , which is the only free geometric parameter. Hence all the results will be presented as functions of  $\kappa$ .

A Galerkin expansion is used for discretizing the PDEs of motion. As the eigenmodes  $\Phi_p(r, \theta)$  are known analytically [44], they are used for expanding the unknown transverse displacement:

$$w(r, \theta, t) = \sum_{p=1}^{+\infty} X_p(t) \Phi_p(r, \theta). \quad (18)$$

The modal displacements  $X_p$  are the unknowns, and their dynamics is governed by,  $\forall p \geq 1$ :

$$\ddot{X}_p + 2\xi_p\omega_p\dot{X}_p + \omega_p^2 X_p + \varepsilon_q \sum_{i,j=1}^{+\infty} \tilde{g}_{ij}^p X_i X_j + \varepsilon \sum_{i,j,k=1}^{+\infty} \tilde{h}_{ijk}^p X_i X_j X_k = 0. \quad (19)$$

The analytical expressions for the quadratic and cubic coupling coefficients ( $\tilde{g}_{ij}^p, \tilde{h}_{ijk}^p$ ) involve integrals of products of eigenmodes on the surface, they can be found in [44, 22]. As in the previous section, a modal viscous damping term of the form  $2\xi_p\omega_p\dot{X}_p$  is considered, whereas external forces has been cancelled as only free responses are studied.

The type of non-linearity can be inferred from Eqs (19) by using the NNM method. The results for an undamped shell has already been computed and are presented in [22]. However, an extension of the NNM-method, taking into account the damping term, has been proposed in [39]. Amongst other things, it has been shown on a simple two-dofs system of coupled oscillators, that the type of non-linearity depends on the damping. The aim of this section is thus to complement the results presented in [22] for documenting the dependence of a shell on viscous damping and for assessing its effect.

## 4.2 Numerical results

Three cases are selected in order to derive results for a variety of damping behaviours:

**case (i)**  $\forall p = 1 \dots N, \xi_p = \xi / \omega_p$

**case (ii)**  $\forall p = 1 \dots N, \xi_p = \xi$

**case (iii)**  $\forall p = 1 \dots N, \xi_p = \xi \omega_p$

where  $\xi$  is a constant value, ranging from 0 to 0.3. Case (i) corresponds to a decay factor ( $2\xi_p\omega_p = 2\xi$ ) that is independent from the frequency, *i.e.* with a constant  $2\xi$  value for any mode. With a small value of  $\xi$ , it may model the low-frequency (*i.e.* below the critical frequency) behaviour of thin metallic structures such as aluminium plates [45, 46]. Case (ii) describes a decay factor that is linear with the frequency, and may model for instance damped structures as glass plates in the low-frequency range [45]. Finally, case (iii) accounts for a strongly damped structure, with a center manifold limited to a few modes.

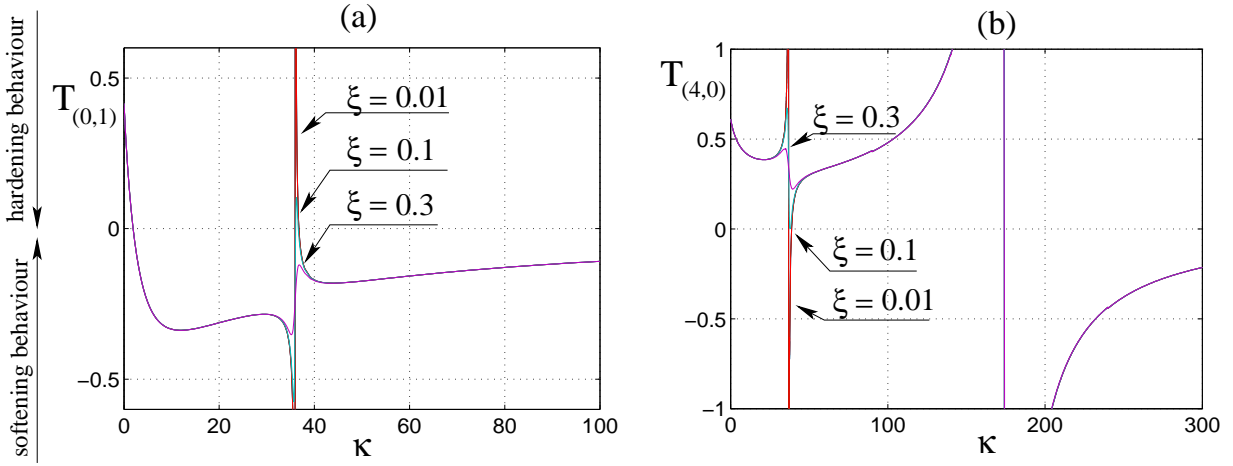


Figure 11: Type of non-linearity for (a): mode (0,1) and (b): (4,0) versus the aspect ratio  $\kappa$  of a shallow spherical shell. Increasing values of damping for case (i) ( $\forall p = 1 \dots N, \xi_p = \xi / \omega_p$ ), are shown, with  $\xi = 0$  and 0.01 (red), 0.1 (cyan) and 0.3 (violet).

The effect of increasing damping is shown for modes (0,1) and (4,0), for case (i) in Fig. 11, case (ii) in Fig. 12, and case (iii) in Fig. 13. Mode (0,1) undergoes a rapid change of behaviour: the transition from hardening to softening type non-linearity occurs at  $\kappa = 1.93$ . Then 2:1 internal resonance with mode (0,2) occurs at  $\kappa = 36$ , but the behaviour remains of the softening type. Mode (4,0) displays a hardening behaviour until the 2:1 resonance with mode (0,1) at  $\kappa = 174.1$ . The first resonance with (0,2) at  $\kappa = 36.9$  does not change the behaviour on a large interval. Adding the damping of case (i) shows that the discontinuity occurring at 2:1 internal resonance is smoothed. However, it happens for a quite large amount of damping in the structure. Damping values of 0,  $1e-4$ ,  $1e-3$  and  $1e-2$  have been tested and give exactly the same behaviour so that only one curve is visible in Fig. 11. Large values of the damping term  $\xi$ , namely 0.1 and 0.3 (which correspond to strongly damped structures) must be selected to see the discontinuity smoothed. Moreover, outside the narrow intervals where 2:1 resonance occurs, the effect of damping is not visible. As a conclusion for case (i), it appears that this kind of damping has a really marginal effect on the type of non-linearity, so that undamped results can be estimated as reliable for lightly damped structures with modal damping factor below 0.1.



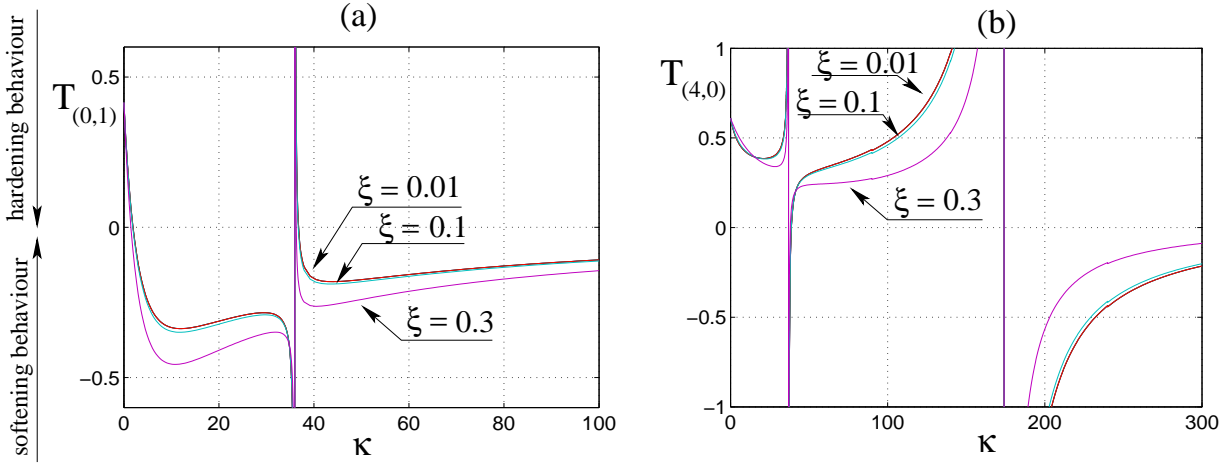


Figure 12: Type of non-linearity for (a): mode (0,1) and (b): (4,0) versus the aspect ratio  $\kappa$ . Increasing values of damping for case (ii) ( $\forall p = 1 \dots N, \xi_p = \xi$ ), are shown, with  $\xi = 0$  and 0.01 (red), 0.1 (cyan) and 0.3 (violet).

Case (ii) corresponds to a more damped structure than case (i). However, it is observed in Fig. 12 that the discontinuity is not smoothed at the 2:1 internal resonance. Inspecting back the analytical results show that this is a natural consequence of the expression of the coefficients of the non-linear change of co-ordinates for asymptotic NNMs. When the specific case of constant damping factors is selected, small denominators remain present. On the other hand, outside the regions of 2:1 resonance, the effect of damping is pronounced and enhances the softening behaviour. But once again, very large values of damping factors such as 0.3 must be reached to see a prominent influence.

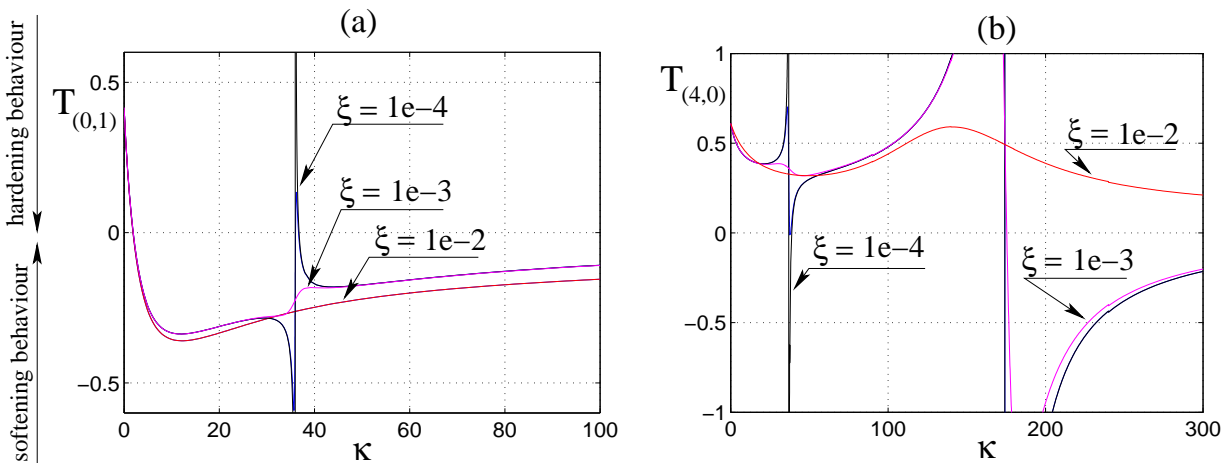


Figure 13: Type of non-linearity for (a): mode (0,1) and (b): (4,0) versus the aspect ratio  $\kappa$ . Increasing values of damping for case (iii) ( $\forall p = 1 \dots N, \xi_p = \xi \omega_p$ ), are shown, with  $\xi = 0$  and 1e-4 (black), 1e-3 (magenta) and 1e-2 (red).

Finally, case (iii) depicts the case of a rapidly increasing decay factor with respect to the frequency. As the overall damping in the structure is thus larger, smaller values of  $\xi$  have been selected,

namely  $1e-4$ ,  $1e-3$  and  $1e-2$ .  $\xi = 1e-4$  gives quite coincident results with  $\xi = 0$ . But from  $\xi = 1e-3$ , the effect of the damping is very important: the discontinuities are smoothed, except the larger one occurring for mode (4,0) with mode (0,1). For  $\xi = 1e-2$ , 2:1 resonance are not visible anymore. A particular result with this value is for mode (4,0): the smoothing effect is so important that the non-linearity remains of the hardening type. Finally, the fact that the damping generally favours the softening behaviour can not be declared as a general rule, as one counterexample has been exhibited here. From these results, it can be inferred that the damping has little incidence on the type of non-linearity for thin structures, until very large values are attained. It is observed that the damping generally favours the softening behaviour, but this rule is not true in general. In particular when the transition from hardening to softening type non-linearity is due to a 2:1 internal resonance, and is not the direct effect of the change of geometry, a large value of damping may favour hardening behaviour, as observed here for mode (4,0) in case (iii).

## 5 Conclusion

The effect of geometric imperfections on the hardening/softening behaviour of circular plates with a free edge has been studied. Thanks to the NNMs, quantitative results for the transition from hardening to softening behaviour has been documented, for a number of modes and for two typical imperfections. Two general rules have been observed from the numerical results: for modes which eigenfrequency strongly depends on the imperfection, the type of non-linearity changes rapidly, and softening behaviour occurs for a very small imperfection with an amplitude being a fraction of the plate thickness. On the other hand, some eigenfrequencies show a slight dependence with the considered imperfection. For these, 2:1 internal resonances are the main factor for changing the type of non-linearity. In a second part of the paper, the effect of viscous damping on the type of non-linearity of shallow spherical shells have been studied. It has been shown quantitatively that this effect is slight for usual damping values encountered in thin structures.

## References

- [1] S. A. Tobias. Free undamped non-linear vibrations of imperfect circular disks. *Proc. of the Instn. of Mech. Eng.*, 171:691–700, 1957.
- [2] N. Yamaki. Influence of large amplitudes on flexural vibrations of elastic plates. *ZAMM*, 41(12):501–510, 1961.
- [3] K. A. V. Pandalai and M. Sathyamoorthy. On the modal equations of large amplitude flexural vibration of beams, plates, rings and shells. *International Journal of Non-linear Mechanics*, 8(3):213–218, 1973.
- [4] S. Sridhar, D. T. Mook, and A. H. Nayfeh. Non-linear resonances in the forced responses of plates, part I: symmetric responses of circular plates. *Journal of Sound and Vibration*, 41(3):359–373, 1975.
- [5] C. Touzé, O. Thomas, and A. Chaigne. Asymmetric non-linear forced vibrations of free-edge circular plates, part I: theory. *Journal of Sound and Vibration*, 258(4):649–676, 2002.

- [6] O. Thomas, C. Touzé, and A. Chaigne. Asymmetric non-linear forced vibrations of free-edge circular plates, part II: experiments. *Journal of Sound and Vibration*, 265(5):1075–1101, 2003.
- [7] P. L. Grossman, B. Koplik, and Y-Y. Yu. Nonlinear vibrations of shallow spherical shells. *ASME Journal of Applied Mechanics*, 39E:451–458, 1969.
- [8] D. Hui. Large-amplitude vibrations of geometrically imperfect shallow spherical shells with structural damping. *AIAA Journal*, 21(12):1736–1741, 1983.
- [9] K. Yasuda and G. Kushida. Nonlinear forced oscillations of a shallow spherical shell. *Bull. JSME*, 27(232):2233–2240, 1984.
- [10] D. Hui. Large-amplitude axisymmetric vibrations of geometrically imperfect circular plates. *Journal of Sound and Vibration*, 2(91):239–246, 1983.
- [11] A. H. Nayfeh, J. F. Nayfeh, and D. T. Mook. On methods for continuous systems with quadratic and cubic nonlinearities. *Nonlinear Dynamics*, 3:145–162, 1992.
- [12] C. Touzé, O. Thomas, and A. Chaigne. Hardening/softening behaviour in non-linear oscillations of structural systems using non-linear normal modes. *Journal of Sound and Vibration*, 273(1-2):77–101, 2004.
- [13] M. Amabili, F. Pellicano, and M. P. Païdoussis. Non-linear vibrations of simply supported, circular cylindrical shells, coupled to quiescent fluid. *Journal of Fluids and Structures*, 12:883–918, 1998.
- [14] E. H. Dowell. Comments on the nonlinear vibrations of cylindrical shells. *Journal of Fluids and Structures*, 12(8):1087–1089, 1998.
- [15] M. Amabili, F. Pellicano, and M. P. Païdoussis. Further comments on nonlinear vibrations of shells. *Journal of Fluids and Structures*, 13(1):159–160, 1999.
- [16] D. A. Evensen. Nonlinear vibrations of cylindrical shells – logical rationale. *Journal of Fluids and Structures*, 13(1):161–164, 1999.
- [17] M. Amabili and M. P. Païdoussis. Review of studies on geometrically non-linear vibrations and dynamics of circular cylindrical shells and panels, with and without fluid-structure interactions. *ASME Applied Mechanics Review*, 56(4):349–381, 2003.
- [18] M. Amabili. *Nonlinear vibrations and stability of shells and plates*. Cambridge University Press, 2008.
- [19] G. Rega, W. Lacarbonara, and A. H. Nayfeh. Reduction methods for nonlinear vibrations of spatially continuous systems with initial curvature. *Solid Mechanics and its applications*, 77:235–246, 2000.
- [20] F. Pellicano, M. Amabili, and M. P. Païdoussis. Effect of the geometry on the non-linear vibration of circular cylindrical shells. *International Journal of Non-linear Mechanics*, 37:1181–1198, 2002.

- [21] H. N. Arafat and A. H. Nayfeh. Non-linear responses of suspended cables to primary resonance excitation. *Journal of Sound and Vibration*, 266:325–354, 2003.
- [22] C. Touzé and O. Thomas. Non-linear behaviour of free-edge shallow spherical shells: effect of the geometry. *International Journal of Non-linear Mechanics*, 41(5):678–692, 2006.
- [23] A. Rosen and J. Singer. Effect of axisymmetric imperfections on the vibrations of cylindrical shells under axial compression. *AIAA Journal*, 12:995–997, 1974.
- [24] D. Hui and A. W. Leissa. Effects of uni-directional geometric imperfections on vibrations of pressurized shallow spherical shells. *International Journal of Non-linear Mechanics*, 18(4):279–285, 1983.
- [25] P. B. Gonçalves. Axisymmetric vibrations of imperfect shallow spherical caps under pressure loading. *Journal of Sound and Vibration*, 174(2):249–260, 1994.
- [26] M. Amabili. A comparison of shell theories for large-amplitude vibrations of circular cylindrical shells: Lagrangian approach. *Journal of Sound and Vibration*, 264:1091–1125, 2003.
- [27] V. D. Kubenko and P. S. Koval’chuk. Influence of initial geometric imperfections on the vibrations and dynamic stability of elastic shells. *International Applied Mechanics*, 40:847–877, 2004.
- [28] E. L. Jansen. The effect of geometric imperfections on the vibrations of anisotropic cylindrical shells. *Thin-Walled Structures*, 45:274–282, 2007.
- [29] C.-Y. Chia. Non-linear free vibration and postbuckling of symmetrically laminated orthotropic imperfect shallow cylindrical panels with two adjacent edges simply supported and the other edges clamped. *International Journal of Solids and Structures*, 23(8):1123–1132, 1987.
- [30] D. Hui and A. W. Leissa. Effects of geometric imperfections on vibrations of biaxially compressed rectangular flat plates. *ASME Journal of Applied Mechanics*, 50:750–756, 1983.
- [31] N. Yamaki, K. Otomo, and M. Chiba. Non-linear vibrations of a clamped circular plate with initial deflection and initial edge displacement, part i: Theory. *Journal of Sound and Vibration*, 79:23–42, 1981.
- [32] N. Yamaki, K. Otomo, and M. Chiba. Non-linear vibrations of a clamped circular plate with initial deflection and initial edge displacement, part i: Experiment. *Journal of Sound and Vibration*, 79:43–59, 1981.
- [33] N. Yamaki and M. Chiba. Non-linear vibrations of a clamped rectangular plate with initial deflection and initial edge displacement, part i: Theory. *Thin-Walled Structures*, 1(1):3–29, 1983.
- [34] N. Yamaki, K. Otomo, and M. Chiba. Non-linear vibrations of a clamped rectangular plate with initial deflection and initial edge displacement, part ii: Experiment. *Thin-Walled Structures*, 1(1):101–119, 1983.
- [35] M. Amabili. Theory and experiments for large-amplitude vibrations of rectangular plates with geometric imperfections. *Journal of Sound and Vibration*, 291(3-5):539–565, 2006.

- [36] M. Amabili. Theory and experiments for large-amplitude vibrations of empty and fluid-filled circular cylindrical shell with imperfections. *Journal of Sound and Vibration*, 262(4):921–975, 2003.
- [37] M. Amabili. Theory and experiments for large-amplitude vibrations of circular cylindrical panel with geometric imperfections. *Journal of Sound and Vibration*, 298:43–72, 2006.
- [38] C. C. Lin and L. W. Chen. Large-amplitude vibration of an initially imperfect moderately thick plate. *Journal of Sound and Vibration*, 135(2):213–224, 1989.
- [39] C. Touzé and M. Amabili. Nonlinear normal modes for damped geometrically non-linear systems: application to reduced-order modelling of harmonically forced structures. *Journal of Sound and Vibration*, 298(4-5):958–981, 2006.
- [40] G. J. Efstathiades. A new approach to the large-deflection vibrations of imperfect circular disks using Galerkin’s procedure. *Journal of Sound and Vibration*, 16(2):231–253, 1971.
- [41] G. L. Ostiguy and S. Sassi. Effects of initial geometric imperfections on dynamic behaviour of rectangular plates. *Non-linear Dynamics*, 3:165–181, 1992.
- [42] C. Camier, C. Touzé, and O. Thomas. Non-linear vibrations of imperfect free-edge circular plates. *European Journal of Mechanics, A/Solids*, submitted, 2007.
- [43] C. Camier, C. Touzé, and O. Thomas. Effet des imperfections géométriques sur les vibrations non-linéaires de plaques circulaires minces. In *18ème Congrès Français de Mécanique*, Grenoble, France, August 2007.
- [44] O. Thomas, C. Touzé, and A. Chaigne. Non-linear vibrations of free-edge thin spherical shells: modal interaction rules and 1:1:2 internal resonance. *International Journal of Solids and Structures*, 42(11-12):3339–3373, 2005.
- [45] A. Chaigne and C. Lambourg. Time-domain simulation of damped impacted plates. I: Theory and experiments. *Journal of the Acoustical Society of America*, 109(4):1422–1432, 2001.
- [46] M. Amabili. Nonlinear vibrations of rectangular plates with different boundary conditions: theory and experiments. *Computers and Structures*, 82(31-32):2587–2605, 2004.